Food and Bioprocess Technology (2023) 16:2001–2015
https://doi.org/10.1007/s11947-023-03048-7

RESEARCH

Carrageenan/Alginate-Based Functional Films Incorporated with *Allium sativum* Carbon Dots for UV-Barrier Food Packaging

Ajahar Khan[1] · Ruchir Priyadarshi[1] · Tanima Bhattacharya[1] · Jong-Whan Rhim[1]

Received: 16 November 2022 / Accepted: 23 February 2023 / Published online: 4 March 2023

Abstract

Hydrothermally prepared garlic (*Allium sativum*) cloves-derived carbon dots (CDs) were used to fabricate carrageenan/sodium alginate (Car/Alg)-based functional films for UV-barrier food packaging. The effects of different concentrations of CDs on the films' structural, functional, physical, and mechanical properties were analyzed. The CDs acted as a reinforcing agent to improve the films' mechanical stability and surface hydrophobicity. The structural characterization indicated good compatibility between CDs and the Car/Alg polymer matrix. The functional films showed a significant bacteriostatic effect against foodborne pathogenic bacteria *E. coli* and *L. monocytogenes*. Besides, they exhibited excellent UV-blocking properties (~85.1% in the UV-A and 99.0% in the UV-B). In addition, CD-incorporated Car/Alg films showed high antioxidant activity as determined by ABTS (98.6 ± 0.3%) and DPPH (34.2 ± 0.3%) free radical scavenging methods. When used for UV protection packaging of raw meat, the functional film could preserve the meat color even when directly exposed to UV light for 30 h. The results indicate the potential of CD-containing Car/Alg-based films for active food packaging applications, especially as UV-blocking films for preserving the visual quality of meat products.

Keywords Carbon dots · Biopolymers · UV barrier · Antioxidant · Antimicrobial · Food packaging

Introduction

The demand for processed and packaged foods is growing exponentially with the rapidly changing human lifestyle around the world. The food industry is constantly striving to meet consumer demand for safe and convenient food. The market is overwhelmed with processed foods at different stages, from minimally processed products to heated foods. Preservation and packaging of pre-cooked and heated foods have advanced considerably, but the preservation of minimally processed foods such as fresh fruit and sliced raw meat still has a long way to go. Minimally processed meat products are one of the most commonly consumed, short-lived perishables, easily spoiled during storage, and distribution, and require specialized packaging and preservation techniques.

During shelf life, raw meat products, especially on illuminated supermarket shelves, can be photodegraded and photo-oxidized by UV light, which can degrade quality (Csapó et al., 2019). UV exposure leads to the formation of oxidative free radicals, which accelerate the breakdown of food, leading to rancidity, off-flavors, discoloration of food, and reduced dietary value (Bosset et al., 1994; Csapó et al., 2019). Main food components that are impacted by UV radiations, typically identified as photosensitizers, include vitamins and typical food colorants such as oils, fats, chlorophylls, and myoglobin (Duncan & Hannah, 2012; Kwon et al., 2018). Not only is it decomposed by UV rays, but it is also easily contaminated by microorganisms, especially psychotropic bacteria such as *Listeria*, which is one of the leading causes of foodborne diseases. The World Health Organization (WHO) estimates that in 2015, 600 million people were affected by food pollution, and 420,000 people die each year from foodborne diseases (Bahrami et al., 2020; Hoelzer et al., 2018). Additionally, more than 550 million diseases are caused by diarrheal infections, primarily from eating contaminated food (Yousefi et al., 2019). Therefore, impending new practices to prevent the spoilage of meat products are essential. In this regard, food packaging is practiced throughout the food supply to ease the handling, improve shelf life, organoleptic characteristics, ergonomics,

✉ Jong-Whan Rhim
jwrhim@khu.ac.kr

[1] Department of Food and Nutrition, BioNanocomposite Research Center, Kyung Hee University, 26 Kyungheedae-ro, Dongdaemun-gu, Seoul 02447, South Korea

and flexibility, and reduce physicochemical changes in color, flavor, weight, bioavailability, texture, and moisture content (Jafari et al., 2018; Mousavi-Khaneghah et al., 2018) as well as safety against both chemical and microbiological contaminations (Fathima et al., 2018). Nanomaterials, such as metal nanoparticles and carbon dots, possess excellent antibacterial efficacy against various microbial strains due to their exclusive physicochemical properties, such as structural defects, surface charge, small size, and functional groups (Khan et al., 2023; Makvandi et al., 2020; Soltani-Firouz et al., 2021). Moreover, nanomaterials have also been reported for their promising antioxidant efficacy. The antioxidant agents in the food scavenge or neutralize the unfavorable compounds such as oxygen, metal ions, or radical oxidative species generated during food storage (Ezati et al., 2022a). Therefore, to ensure food safety, an appropriate packaging technology comprising suitable antibacterial and antioxidants plays an essential role in reducing oxidation and contamination of food, extending shelf life, maintaining food safety, and preserving food quality (Mei et al., 2022; Sivakanthan et al., 2020). Biopolymers combined with functional nanomaterials have been widely studied for their potential to replace non-degradable plastic packaging materials (Malik & Mitra, 2021; Perera et al., 2022).

Carbon dots (CDs), a new member of carbon nanomaterials, have very good chemical and photochemical stability and exclusively possess the main properties of semiconductor quantum dots (QDs) (Min et al., 2022). CD has emerged as a promising candidate in the field of carbon nanomaterials due to its high fluorescence, good photoluminescence (PL), hydrophilicity, good biocompatibility, and low toxicity (Saini et al., 2022). These properties are evident as powerful advantages in the context of biological applications and thus represent a natural alternative to conventional QDs as they exhibit relatively similar or better performance (Đorđević et al., 2022). In the past few years, the CD has been exploited with huge potential in several areas, such as photocatalysis, solar energy harvesting, light-emitting diodes, antibacterial activity, antioxidant activity, chemical sensing, and bioimaging (Saini et al., 2022; Wang & Qiu, 2016; Zu et al., 2017). CDs have been used as sustainable, safe, and non-toxic fillers in food packaging polymers. When used as fillers, they impart high antioxidant and antimicrobial properties to the food packaging materials, thus aiding and enhancing the packed food shelf life (Ezati et al., 2022a). Besides, several studies have reported the synthesis of CDs from sustainable sources for use in food packaging applications.

Furthermore, CDs are better than other functional additives in food packaging. Being derived from agro-waste materials, they are more economical than other chemically derived nanomaterials, such as metal oxides which are generally used in food packaging (Ezati et al., 2022b). Additionally, due to their natural origin, they possess high biocompatibility and non-toxicity, which are major issues with chemically synthesized nanomaterials (Ezati et al., 2022b).

It has been investigated that the coating of CD improved the microbial and physicochemical quality of fresh-cut cucumber, affecting total bacterial count, yeast and mold, weight loss, firmness, respiration rate, total soluble solids, peroxidases activity, malondialdehyde content, polyphenol oxidase activity, taste, flavor, and water status during storage (Fan et al., 2020). Furthermore, coating of chitosan-impregnated CDs effectively controlled gas composition (low O_2 and high CO_2 concentrations), maintained a minimum weight loss of 4.1%, inhibited aerobic bacterial growth, and reduced flavor loss in the fresh-cut cucumbers during storage (Fan et al., 2021). Additionally, the addition of CDs enhances the film's functionality, making it a potential replacement for traditional packaging (Zhang et al., 2017).

Nonetheless, the properties of a CD vary depending on its source and composition. Therefore, it is necessary to evaluate the properties of CDs in food packaging applications. One natural source for synthesizing sustainable CDs is garlic (*Allium sativum*). Garlic is a representative functional food containing various flavonoids and other active compounds, and garlic CD is assumed to have good functionality. Garlic is known to have strong anticancer, antifungal, antimicrobial, antioxidant, antibacterial, and anti-viral properties (Kalkal et al., 2021).

To date, synthetic plastics are most commonly used in commercial food packaging due to their cost-effectiveness and superior performance. However, the ever-growing adverse environmental impacts and non-biodegradability raise significant concerns about using these economical and easy-to-use polymeric materials (Motelica et al., 2020; Schmaltz et al., 2020; Souza et al., 2015). Adopting suitable biopolymers to manufacture active packaging films is important to improve and maintain food quality, such as nutrients, color, texture, etc., and to reduce microbial contamination. Microorganisms carry out the most important biopolymer biodegradation activities, such as hydrolysis of ester linkages to release monomers, eventually producing end products of carbon dioxide and water under aerobic conditions. On the other hand, abiotic processes such as photolysis and chemical hydrolysis are carried out in high-temperature, acidic, or basic environments simultaneously with chemically and physically degraded biopolymers (Polman et al., 2021). For example, Zhou et al. investigated that in soil, the κ-carrageenan film was preserved intact for the first two days, began to deteriorate after day 3, and was completely damaged by day 7 (Zhou et al., 2022). In another study, iota-carrageenan and arrowroot starch were used to create edible films that could degrade completely in a week under composting soil and seawater conditions (Abdillah & Charles, 2021). Santos et al. also reported that after 6 days buried in the sand, the sodium alginate films began to show signs of

fragmentation, being completely degraded in 15 days (Santos et al., 2022). Therefore, the blending of biopolymers to produce biodegradable films has received much consideration due to the superior properties of blended polymers compared to single-polymer films (Kumar et al., 2020; Roy & Rhim, 2021). Therefore, a mixture of carrageenan and sodium alginate biopolymer was adopted, which seems to be a good combination for making active packaging films.

Sodium alginate (Alg) is a biocompatible and non-toxic natural linear block copolymer comprised of β-D-mannuronic and α-l-guluronic acid residues linked by a β-(1–4) glycosidic bond (Nasrollahzadeh et al., 2021). Generally, films fabricated using alginate possess good flexibility with decent tensile strength and oxygen barrier properties, which are advantageous attributes for food packaging (Shahabi-Ghahfarrokhi et al., 2020). On the other hand, κ-carrageenan (Car) is a water-soluble marine polysaccharide extracted from red seaweeds (Fouda et al., 2015). Chemically, its structure involves the repetition of disaccharide units: 4-linked 3,6-anhydro-α-D-galactose and 3-linked-β-D-galactose-4-sulfates (Fouda et al., 2015; Hashemi et al., 2018). Both Alg and κ-Car have been widely used in the manufacture of biodegradable packaging films because of their good film-forming ability, mechanical properties, and limited water sensitivity (Liu et al., 2019; Meng et al., 2014; Puscaselu et al., 2020).

This study aims to develop active packaging applications, including Car/Alg-based functional films on garlic (*Allium sativum*)-derived CDs. The effect of CD incorporation on the UV blocking, antioxidant, antibacterial, mechanical, optical, water vapor permeability, and surface wettability of the Car/Alg blend matrix was also evaluated. The fabricated UV-blocking film was applied to beef packaging to quantitatively and qualitatively evaluate the possibility of preventing meat discoloration.

Experimental

Materials and Methods

Sodium alginate (Alg) and carrageenan (Car) (κ-carrageenan, HE-A, viscosity: 50 cps in 1.5% aqueous solution at 75 °C) were procured from Kanto Chemical Co., Inc. (Tokyo, Japan) and Hankook Carragen (Jeonnam, Korea), respectively. Potassium persulfate, 2,2-diphenyl-1-picrylhydrazyl (DPPH), and 2,2′-azino-bis(3-ethylbenzothiazoline-6-sulfonic acid) (ABTS) were supplied by Sigma-Aldrich (St. Louis, MO, USA). Glycerol was obtained from Daejung Chemicals & Metals Co., Ltd. (Siheung, Gyeonggi-do, Korea). Foodborne pathogenic bacteria *E. coli* O157: H7 ATCC 43895 and *L. monocytogenes* ATCC 15313 were provided by the Korean Collection for Type Culture (KCTC, Seoul, Korea). Brain heart infusion broth (BHI), tryptic soy broth (TSB), and agar powder were procured from Duksan Pure Chemicals Co., Ltd. (Ansan, Gyeonggi-do, South Korea) and were adopted for bacterial culture. All the other chemicals were used directly without additional purification. Fresh red meat (beef) was purchased from a local supermarket in Seoul, Korea.

Synthesis of CDs

The CDs were prepared by a well-known, one-pot facile hydrothermal approach utilizing garlic as a carbon precursor, as shown in Fig. 1 (Ezati et al., 2022a). In a simple procedure, 2 g of garlic cloves was washed with double distilled water (DW), followed by crushing in mortar and pestle. This crushed garlic paste was mixed with 50 mL DW under mechanical agitation, transferred to a Teflon-lined cylinder (100 mL), and sealed in a stainless steel reactor. The reactor was placed in an oil bath at 200 °C for 6 h. After natural cooling to room temperature, the larger particles in the solution were removed through centrifugation (8000 rpm for 20 min) and filtering through a Whatman membrane filter (pore size: 0.22 µm). The prepared CDs were purified by dialysis (Spectra/Por® 7 Dialysis Membrane, Spectrum Laboratories, Inc. USA, nominal flat width: 18 mm, diameter: 11.5 mm, vol/length: 1.1 mL/cm) and kept at 4 °C until further characterization.

Characterization of CDs

The absorption spectrum of the CDs (0.01 wt% in distilled water) was recorded using a UV–vis spectrophotometer (Mecasys Optizen POP Series UV/Vis, Seoul, Korea) in the range of 200–600 nm at 25 °C. The fluorescent emission behavior under different excitation wavelengths was recorded on a fluorescence spectrophotometer (F-7100 FL, Hitachi, Japan) at 25 °C. The maximum fluorescent emission response was attained by varying the excitation wavelength from 330 to 430 nm with an increment of 10 nm. The slit width and scan speed were fixed at 5 nm and 1200 nm/min, respectively. Transmission electron microscopy (TEM) (FE-TEM, JEM-2100F, Jeol Ltd., Tokyo, Japan) was employed to demonstrate the hierarchical morphology, including the shape and size of the synthesized CDs. The testing sample for TEM analyses was developed on a copper grid with carbon coating by dropping the aqueous CDs dispersion followed by drying at 25 °C. The average particle size and size distribution were determined using ImageJ software (ImageJ 1.53 k Wayne Rasband and Contributors, National Institute of Health, USA). The surface charge and stability of CDs in an aqueous medium were evaluated using a zeta potential analyzer (Zetasizer Nano ZS-ZEN 3600, Malvern Instruments Ltd., UK).

Fig. 1 Schematic illustration of the fabrication of the sodium alginate (Alg), carrageenan (Car), and carbon dots (CD) based Car/Alg, Car/Alg-CD$^{1\%}$, Car/Alg-CD$^{2\%}$, Car/Alg-CD$^{3\%}$, and Car/Alg-CD$^{4\%}$ films

Preparation of Car/Alg Bionanocomposite Films

The CD-dispersed composite polymer films were fabricated using the solution casting method shown in Fig. 1 while increasing the CD content in the carrageenan/sodium alginate (Car/Alg)-based binary composite. Briefly, 1% (w/v) of each Car and Alg were added into a beaker comprising 200 mL of DW and 30% (w/v) plasticizer, i.e., glycerol (1.2 g concerning the weight of Car/Alg binary composite) and mixed thoroughly with a magnetic stirrer for 90 min at 85 °C. The homogenous binary composite mixture was cooled to 50 °C. Subsequently, the predetermined amount of synthesized CDs (1 to 4 wt% of Car/Alg) was added to the obtained solution mixture under constant stirring at 50 °C for 2 h. The resultant viscous solution mixtures (200 mL) were cast manually on Teflon-coated glass plates (24 × 30 cm^2) and left for drying at 25 °C till complete evaporation of solvents. The dried films were peeled off from the casting plates and stored in a humidity chamber for conditioning at 25 °C and 50% relative humidity (RH) for at least 72 h before further testing. The pristine Car/Alg binary polymer composite film (control) was prepared following the same approach. The fabricated films were designated as Car/Alg, Car/Alg-CD$^{1\%}$, Car/Alg-CD$^{2\%}$, Car/Alg-CD$^{3\%}$, and Car/Alg-CD$^{4\%}$ depending on the CD content.

Film Characterization and Properties

Detailed methods for physicochemical characterizations and film properties are explained in the supporting information.

Application of UV-Blocking Films to Prevent Meat Discoloration

A meat packaging test was carried out to study the practicality of the UV-blocking application of the films. For this, 5 g of bright-red beef meat sample was weighed and kept in a sterilized Petri plate (SPL Life Sciences Co. Ltd., South Korea) covered on the top with the fabricated films (exposed to UV light for 5 min before performing the packaging test). The control sample without any film was used for comparison. The films were applied so the UV radiation could only reach the meat sample after passing through them. The packaging experiment was carried out in the laminar airflow safety chamber with the UV lamp. A broad-spectrum UV lamp (SANKYO DENKI G40T10 40W 4FT Fluorescent Germicidal UV Tube, Japan) was used as a UV source, and the distance between the meat samples and the lamp was 0.5 m. All the samples were kept at 20 °C and observed for 30 h for color change by measuring their color properties compared to the initial values using a Chromameter (Konica Minolta CR-400, Tokyo, Japan).

Results and Discussion

The characterization of CD and the visual appearance of the CD-added Car/Alg-based films are shown in Supporting Information.

Field Emission Scanning Electron Microscopy (FE-SEM) Analysis

FE-SEM micrographs display the surface morphology and cross-sectional microstructures of the fabricated Car/Alg

and CDs incorporated Car/Alg-based bionanocomposite films. The neat Car/Alg film surface was slightly rough, curvier, and compact. Precipitates, impurities, or delaminations were not noticed (Fig. 2a). A similar phenomenon was observed in carrageenan and other polysaccharide-based biocomposite films (Rhim, 2012). Adding 1 wt% CD (Car/Alg-CD$^{1\%}$) did not affect the surface morphology, as the film's surface was free from cracks or cavities, demonstrating that the synthesized CDs were compatible with the polymer matrix. The interaction of hydroxyl groups between CD, CAR, and Alg affects the ordered arrangement of the polymer backbones because of the crosslinking process of the films (Santos et al., 2022). After adding 2 wt% CD, the film (Car/Alg-CD$^{2\%}$) seemed much wavier than the neat Car/Alg film. When 3 wt% CDs (Car/Alg-CD$^{3\%}$) were added, some small agglomerates were observed, and the number of granular agglomerates increased with the addition of 4 wt% CDs (Car/Alg-CD$^{4\%}$); however, they were uniformly distributed throughout the polymer matrix. The dispersion of CDs in the polymer matrix was presumed to be because of the hydrogen-bonding interaction between the hydroxyl and carboxyl groups present on the surface of the CDs, Car, and Alg. The granular surface appearance was most likely due to increased CD accumulation in the Car/Alg blend. The cross-sectional image also showed uniform dispersion of fillers in the polymer matrices, indicating good compatibility between CDs and Car/Alg composite. The elemental mapping analysis of the Car/Alg-CD$^{4\%}$ based bionanocomposite film was carried out to observe the distribution of CDs, and the results are shown in Fig. 2b. It can be observed from the mapping images that the distribution of nitrogen and sulfur was uniform on the surface of bionanocomposite film, indicating the uniform dispersion of CDs. However, intense elemental peaks of carbon, oxygen, and sodium are due to the composition of Car and Alg.

FTIR Analysis

FTIR spectra were recorded to demonstrate the functional groups and structure of pure Car/Alg and CD-loaded Car/Alg-based bionanocomposite film samples. In Fig. 3a, the transmittance peaks positioned at 920, 1027, and 1247 cm^{-1} can be ascribed due to the 3,6-anhydro-D-galactose, glycosidic linkage, and ester sulfate stretching of the carrageenan polymer chain, respectively (Mahdavinia et al., 2014). The occurrence of Alg can be assigned by the characteristic peak positioned around 1419 cm^{-1} ascribed due to the symmetrical vibration of carboxylate groups on the Alg backbone (Mahdavinia et al., 2014). As illustrated in Fig. 3a–e for the neat Car/Alg film and CD-incorporated Car/Alg films, the characteristic peak around 3000 to 3500 cm^{-1} was attributed to the stretching vibration of -OH; the peaks around 1617 cm^{-1} assigned the presence of C = C; the peaks at about ~ 2933 and ~ 1419 cm^{-1} were attributed to the stretching vibration modes of C-H and C-N, respectively; and the absorption at 689 cm^{-1} was attributed to the C-S group (Zhao et al., 2015). These peaks overlapped with the similar -OH, C-H, C = C, and C-S stretching vibration of the Car/Alg polymer blend in the same region (Fig. 3a–e) (Kaya et al., 2018). It can be observed from the FTIR spectra that the intensity of the obtained peaks in the spectra of CD-loaded films decreased without altering the frequency regions, confirming the uniform incorporation and compatibility of the CDs with the Car/Alg polymer blends.

XPS Analyses

XPS measurement was performed to understand the chemical state and presence of the main elements in Car/Alg-CD bionanocomposite films. Figure 4a and b show the survey spectra of Car/Alg and Car/Alg-CD$^{4\%}$, confirming the presence of sulfur (S 2p at 168.8 eV), carbon (C 1 s at 286.5 eV), nitrogen (N 1 s 398.5, eV), and oxygen (O 1 s at 532.7 eV), which was consistent with the EDS spectrum (Wang et al., 2020; Zhao et al., 2015). Regarding the high-resolution XPS C1s spectrum of Car/Alg (Fig. 4c), the fits could be resolved into three component peaks positioned at ~ 283.7 eV, ~ 285.4 eV, and ~ 287.4 eV, which are assigned to the C–C/C-H, C-S/C-O, and C = O, respectively. These peaks are mainly from the groups of Car and Alg composites (Huang et al., 2017; Wang et al., 2020). Whereas for the deconvolution XPS C1s spectrum of Car/Alg-CD$^{4\%}$ (Fig. 4d), the fits could be resolved into four component peaks centered around ~ 283 .8, ~ 285.2, ~ 285.6, and ~ 287.3 eV, corresponds to C–C or C-H bond, C-N, C-S/C- O, and O-C-O or C = O (carbonyl), respectively (Wang et al., 2020). Compared to the three peaks, a new peak at the binding energy of ~ 285.2 eV confirmed the successful incorporation of CDs in the Car/Alg-CD bionanocomposite films (Fig. 4d) (Zhao et al., 2015). The deconvoluted XPS O1s spectra showed the three corresponding peaks at binding energies of ~ 531.3 eV, 532.1 eV, and 533.1 eV being assigned to C = O, C–O–C/C-O–H, and O-C-O groups, respectively (Fig. 4e, f). The high-resolution XPS S 2p spectra of Car/Alg and Car/Alg-CD$^{4\%}$ (Fig. 4g, h) were fitted with three prominent peaks at binding energies of ~ 167.9 eV, ~ 168.8 eV, and ~ 169.5 eV, which are associated with the C-S–O, -OSO_3^{2-} (S $2p_{3/2}$), and -OSO_3^{2-} (S $2p_{1/2}$), respectively (Y. Wang et al., 2020). Additionally, the deconvoluted XPS N 1 s spectrum in Fig. 4i displays the three characteristic peaks of 398.4, 399.1, and 399.9 eV assigned due to C-N–C, N-(C)3, and N–H bonds, respectively (Zhao et al., 2015).

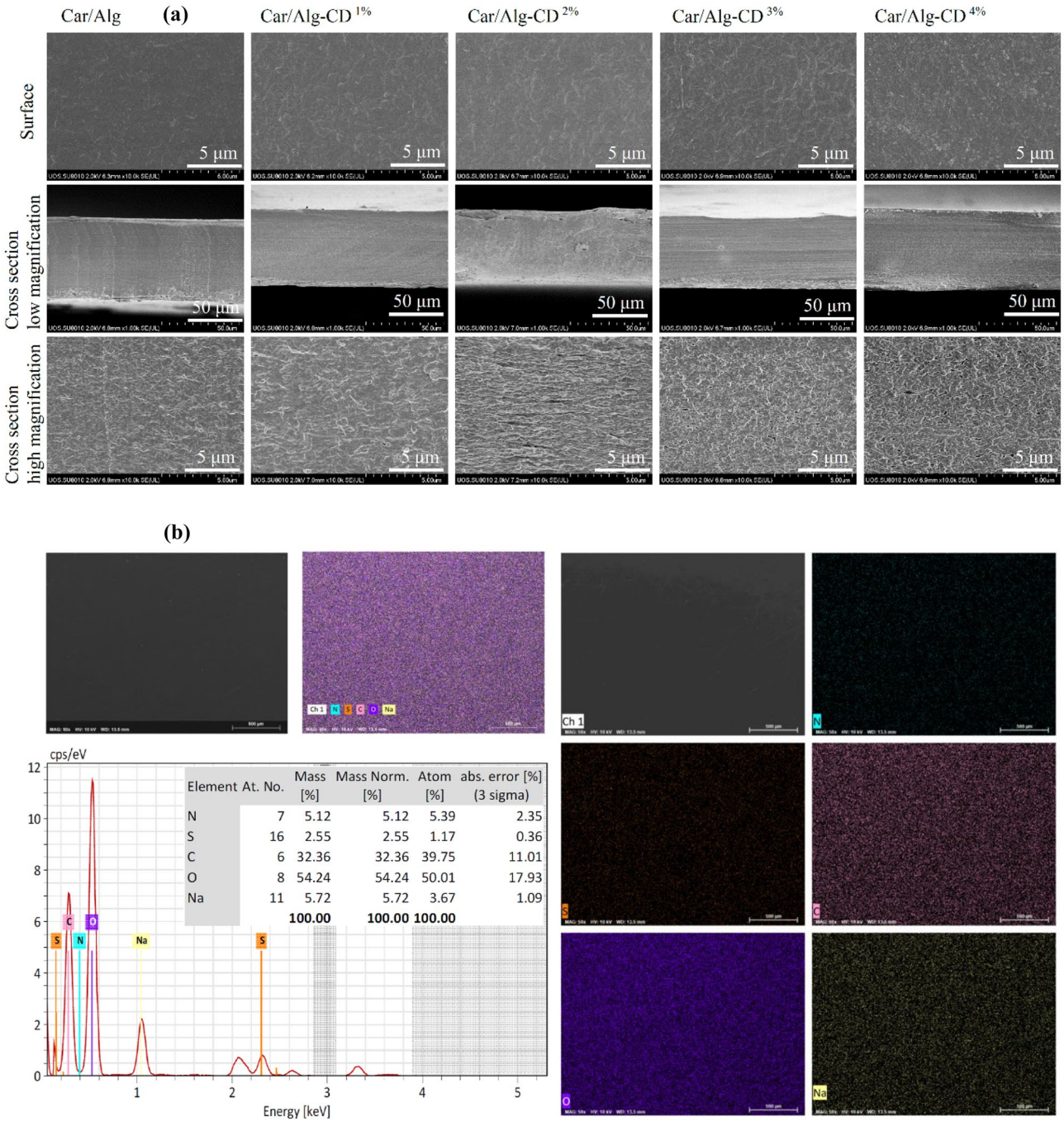

Fig. 2 **a** FE-SEM images showing the surface morphologies and cross-sectional views of the sodium alginate (Alg), carrageenan (Car), and carbon dots (CD) based Car/Alg, Car/Alg-CD$^{1\%}$, Car/Alg-CD$^{2\%}$, Car/Alg-CD$^{3\%}$, and Car/Alg-CD$^{4\%}$ films, and **b** elemental mapping of Car/Alg-CD$^{4\%}$ film

Optical and Color Properties

Transparency and optical properties are vital as they secure visual evidence and satisfy the consumers (Roy et al., 2021). It is well known that the visual appearance of the biopolymer-based active films is altered with the incorporation of an active nanofiller used to impart desired functional properties (Roy et al., 2021). Therefore, it is crucial to determine the color and optical parameters of the fabricated packaging films. The optical properties and color of the Car/Alg-based bionanocomposite films are represented in Table 1. The transparent appearance of neat Car/Alg was significantly decreased with the addition of CDs, which led to a decrease in the brightness (L), followed by increasing the redness (a)

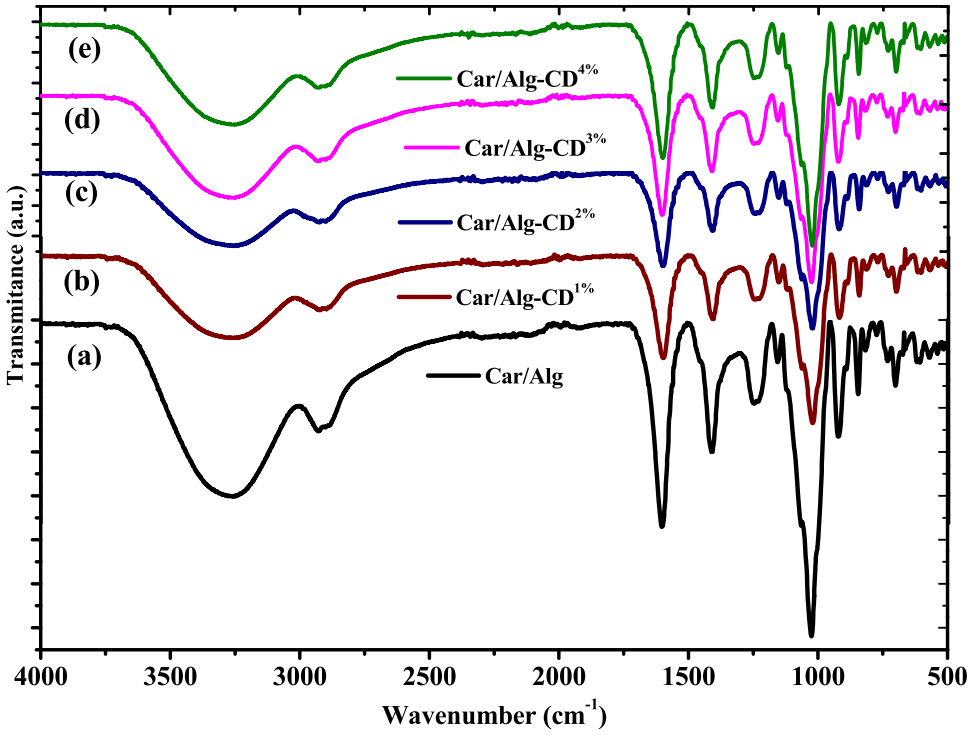

Fig. 3 FTIR spectra of the sodium alginate (Alg), carrageenan (Car), and carbon dots (CD) based **a** Car/Alg, **b** Car/Alg-CD$^{1\%}$, **c** Car/Alg-CD$^{2\%}$, **d** Car/Alg-CD$^{3\%}$, and **e** Car/Alg-CD$^{4\%}$ films

and the yellowness (*b*) of the Car/Alg-CD bionanocomposite films. With the addition of 1, 2, 3, and 4 wt% CDs, the *L* values of the fabricated films reduced with the increase in the concentration of CDs. In contrast, the *a* and *b*-values increased with the concentration due to the yellowish-brown color of the CDs. As a result, the films' total color difference (ΔE) increased significantly. When 4 wt% CDs were added (Car/Alg-CD$^{4\%}$), the film's *a*, *b*, and ΔE values were significantly higher, and the *L*-value was significantly lower than the other films.

UV-Blocking Effect

UV protection of packaging films is an important film property that protects the quality of packaged foods from photochemical reactions (Mathew et al., 2019). Exposure to UV light degrades the food quality and reduces its shelf life through oxidation (Ramos et al., 2012). Furthermore, the quality, nutritional value, and biochemical reactions of food (odor, flavor, and color) are greatly influenced by UV light (< 400 nm) (Duncan & Chang, 2012). Therefore, UV–vis transmission spectra of the neat Car/Alg, Car/Alg-CD$^{1\%}$, Car/Alg-CD$^{2\%}$, Car/Alg-CD$^{3\%}$, and Car/Alg-CD$^{4\%}$ films were thoroughly probed in the UV (200–400 nm), and visible (400–800 nm) ranges (Fig. 5). The neat Car/Alg film showed negligible light absorbance, appearing highly transparent in the visible region, with 85.1 ± 0.2% light transmittance at 660 nm (T_{660}), as shown in Table 1. However, in the UV range, a slight shouldering peak centered at ~ 280 nm for Car/Alg was observed, ascribed to the π-π* transition of the C = O group (carboxylic) of Car/Alg biopolymer. Regarding the UV-shielding characteristic, the neat Car/Alg biocomposite film possessed deficient UV-blocking properties (Fig. 5a, b, Table 1). With the incorporation of CDs into the Car/Alg bionancomposite films, an insignificant decrease in transmittance was noticed for visible light at high wavelength (> 600 nm). On the other hand, a substantial blocking of the light was observed in the low wavelength (400–600 nm) region. Interestingly, a considerable light blockage was observed in the UV region (Fig. 5a, b, Table 1). The UV absorption of the pure Car/Alg film was much smaller than absorption variations between the CD-loaded Car/Alg films fabricated with different concentrations of CDs. This led to the assumption that enhanced UV blocking can be ascribed to an influence of CDs incorporation into the Car/Alg matrix. Interestingly, on the incorporation of 4 wt% CDs, more than 78% of the light was transmitted in the visible region, and the desired blocking was observed in the UV region, i.e., ~ 85.1% in the UV-A region and 99.0% in the UV-B region (Fig. 5b, Table 1). The obtained results demonstrated that the developed sustainable and eco-friendly Car/Alg-CD films were good enough to shield UV-A and UV-B light without any support from semiconducting nanomaterials (Uthirakumar et al., 2018). This UV-blocking efficacy of the packaging films is highly valued to protect the packed food from UV-induced photodegradation.

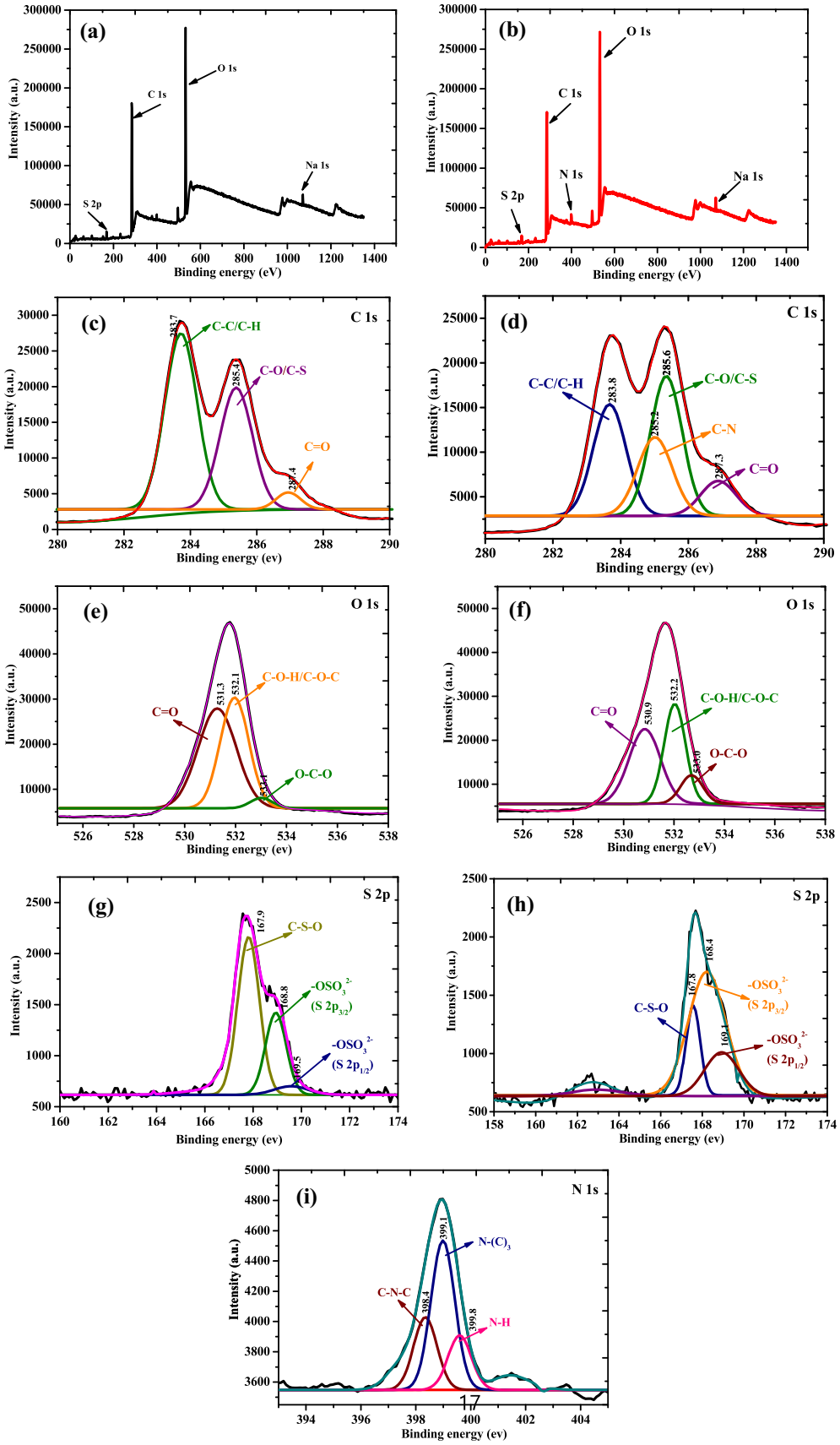
(a)
O 1s
C 1s
Na 1s
S 2p
Intensity (a.u.)
Binding energy (eV)
(b)
O 1s
C 1s
N 1s
S 2p
Na 1s
Intensity (a.u.)
Binding energy (eV)
(c)
C 1s
283.7
C-C/C-H
285.4
C-O/C-S
C=O
289.4
Intensity (a.u.)
Binding energy (ev)
(d)
C 1s
C-C/C-H
283.8
285.6
C-O/C-S
285.2
C-N
289.3
C=O
Intensity (a.u.)
Binding energy (ev)
(e)
O 1s
C=O
531.3
532.1
C-O-H/C-O-C
533.4
O-C-O
Intensity (a.u.)
Binding energy (ev)
(f)
O 1s
C=O
530.9
532.2
C-O-H/C-O-C
534.0
O-C-O
Intensity (a.u.)
Binding energy (eV)
(g)
S 2p
167.9
C-S-O
168.8
-OSO3 2-
(S 2p3/2)
169.5
-OSO3 2-
(S 2p1/2)
Intensity (a.u.)
Binding energy (ev)
(h)
S 2p
167.8
168.4
C-S-O
-OSO3 2-
(S 2p3/2)
169.1
-OSO3 2-
(S 2p1/2)
Intensity (a.u.)
Binding energy (ev)
(i)
N 1s
399.1
N-(C)3
C-N-C
398.3
399.8
N-H
Intensity (a.u.)
Binding energy (ev)

◂**Fig. 4** **a**, **b** XPS full survey spectra, **c**, **d** deconvoluted C1s, **e**, **f** deconvoluted O1s, **g**, **h** deconvoluted S 2p, and **i** deconvoluted N 1 s of the sodium alginate (Alg), carrageenan (Car), and carbon dots (CD) based neat Car/Alg and Car/Alg-$CD^{4\%}$ films, respectively

Mechanical Properties

The mechanical properties of the Car/Alg-based composite films were determined by measuring tensile strength (TS), elongation at break (EB), and elastic modulus (EB), and the results are shown in Table 2. With the incorporation of the CDs, the thickness of the Car/Alg films increased, which varied depending on the concentration of CDs. The neat Car/Alg film was relatively strong and less flexible, with the TS of 45.7 MPa, the EB of 4.5%, and the stiffness (EM) of 2.45 GPa. The mechanical strength of the films significantly increased when CD was incorporated. With the incorporation of 4 wt% of CD, the TS of the Car/Alg film reached 58.6 MPa (28% higher than the neat Car/Alg film), which was attributed to the hydrogen bonding between different functional groups of CDs and Car/Alg polymer matrices. Furthermore, as per the FE-SEM analysis (cross-sectional view), the evenly distributed CDs in the Car/Alg polymer matrices could improve the interfacial interaction and load distribution, resulting in an increased TS. The flexibility (EB) of the films showed an opposite trend to TS values (Priyadarshi & Negi, 2017); however, the difference was not statistically significant ($p > 0.05$). A similar effect of nanofillers on the mechanical properties of different biopolymer-based films has been observed (Priyadarshi et al., 2021b; Roy et al., 2021). Interestingly, the stiffness (EM) did not differ significantly till the incorporation of 2 wt% CDs. However, as the filler concentration was increased further, a significant decrease in the EM was observed, which might be due to the increased aggregation of CDs in the films at higher concentrations due to increased interparticle interaction and decreased interaction with the polymer chains. In previous studies, a similar decrease in the EM was observed in the gelatin-based films when carbon dots concentration was increased above 2% (Min et al., 2022).

Water Vapor Permeability (WVP) and Water Contact Angle (WCA) of the Car/Alg-Based Films

The WVP of the Car/Alg-based films is shown in Table 2. The WVP of the neat Car/Alg film was 1.73×10^{-9} g.m/m^2. Pa.s, consistent with the Car-based active film (Saedi et al., 2021). The incorporation of the CDs slightly reduced the WVP of the Car/Alg-based films, but the decrease was not statistically significant ($p > 0.05$). With the increased incorporation of CDs, the composite films became more compact as the functional groups of the Car/Alg polymer chain were linked to the functional groups of the integrated CD via hydrogen-bonding attraction (Xu et al., 1994). This increased interaction of the polymers with CDs leads to increased interfacial interaction between polymer matrices. However, the decrease in WVP was not statistically significant among the films. Despite the formation of H-bonds, the quantum-sized CDs could not block the free space within the polymer chain and affect the tortuosity of the path for the water molecules. Since the WVP not only depends on the interchain interactions but also the ability of the filler to block the passage of water vapor, the small size of CDs could not create a tortuous path, and the WVP was not reduced significantly. Nevertheless, this hydrogen-bonding interaction between the hydroxyl and carbonyl groups of the Car/Alg polymer matrices with the surface functional groups of the integrated CDs enhanced the overall hydrophobicity of the films.

Table 2 also shows the WCA of the Car/Alg-based composite films. The WCA of the Car/Alg neat film was 45.3°, demonstrating the hydrophilic nature of the control film. The WCA increased from 52.8° to 58.2° as the CD loading increased from 1 to 4 wt%, indicating a strong dependence of the nanofiller amount on decreased surface hydrophilicity of the films. With the addition of CD, the Car/Alg film produced a dense structure and became more hydrophobic (Njuguna et al., 2008). The reason may be that more hydroxyl groups in Car/Alg are attached to CD via hydrogen bonds, which reduces the number of hydrophilic free hydroxyl groups in the polymer matrix, resulting in decreased hydrophilicity (Priyadarshi et al., 2021a; Santos et al., 2021, 2022).

Table 1 Apparent color and light transmittance of the carrageenan/alginate-based composite films

Films	*L*	*a*	*b*	Δ*E*	T_{280} (%)	T_{660} (%)
Car/Alg	90.9 ± 0.1^{e}	-0.5 ± 0.1^{b}	6.4 ± 0.4^{a}	2.6 ± 0.3^{a}	55.4 ± 1.0^{e}	85.1 ± 0.2^{d}
Car/Alg-$CD^{1\%}$	87.8 ± 0.1^{d}	-0.7 ± 0.1^{a}	13.1 ± 0.3^{b}	9.7 ± 0.3^{b}	15.5 ± 0.6^{d}	84.0 ± 0.6^{c}
Car/Alg-$CD^{2\%}$	85.1 ± 0.1^{c}	-0.6 ± 0.1^{ab}	19.7 ± 0.0^{c}	16.8 ± 0.3^{c}	4.0 ± 0.8^{c}	82.4 ± 0.4^{b}
Car/Alg-$CD^{3\%}$	80.5 ± 0.1^{b}	0.7 ± 0.0^{c}	25.2 ± 0.1^{d}	23.8 ± 0.2^{d}	0.7 ± 0.2^{b}	78.4 ± 0.5^{a}
Car/Alg-$CD^{4\%}$	78.9 ± 0.7^{a}	1.2 ± 0.2^{d}	29.3 ± 1.2^{e}	28.7 ± 1.6^{e}	0.6 ± 0.0^{a}	78.4 ± 0.0^{a}

Sodium alginate (Alg), carrageenan (Car), and carbon dots (CD). By Duncan's multiple range tests, means followed by the same letter in the same column were not significant ($p > 0.05$). (*L*: brightness; *a*: redness; *b*: yellowness; Δ*E*: total color difference)

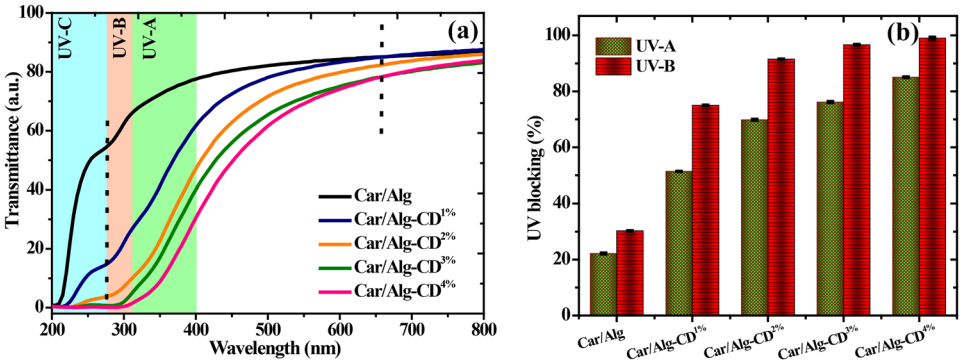

Fig. 5 **a** UV–visible transmittance spectra, **b** plot showing the % UV-A blocking (320–400 nm) and % UV-B blocking (280–320 nm) of the sodium alginate (Alg), carrageenan (Car), and carbon dots (CD) based Car/Alg, Car/Alg-CD$^{1\%}$, Car/Alg-CD$^{2\%}$, Car/Alg-CD$^{3\%}$, and Car/Alg-CD$^{4\%}$ films

Antioxidant Activity

The antioxidant activity of the Car/Alg-based composite films analyzed by the DPPH and ABTS radical scavenging assay is shown in Fig. 6. The ABTS and DPPH free radical scavenging activities of the neat Car/Alg film were 12.3% and 2.3%, respectively. The antioxidant activity of Car/Alg film may be due to the hydroxyl, sulfate, and carboxyl groups in the polymer chain (Sun et al., 2010). However, with the addition of the CDs, the antioxidant activities of the composite films significantly increased depending on the concentration of the CDs. When 1 wt% of CD was added, the ABTS free radical scavenging activity increased significantly to 53.6%, while there was a slight increase in DPPH scavenging activity (3.7%). When 4 wt% of CD were added, the ABTS and DPPH scavenging activity increased to 98.7 ± 0.3% and 34.3 ± 0.3%, respectively (Fig. 6). The difference in antioxidant activity determined by the ABTS and DPPH methods was due to the hydrophilic behavior of the Car/Alg film, which facilitates the release of CDs in the aqueous solution of ABTS compared to the methanolic solution of DPPH (Priyadarshi et al., 2021b). The antioxidant activity of the composite films depended on the concentration of CDs, confirming that the antioxidant activity of the films was mainly due to the CDs. The antioxidant activity of fresh garlic (*Allium sativum)* is well known and mainly due to pungent and unstable organosulfur compounds (Lanzotti, 2006; Rabinkov et al., 1998). Allicin, diallyl trisulfide, and diallyl disulfide in garlic are the major antioxidant compounds (Capasso, 2013; Kim et al., 1997). The results suggest that bioactive composite films with antioxidant CD could potentially be applied to prevent peroxidation, especially in high-fat foods.

Antimicrobial Activity

The antimicrobial potential of the Car/Alg-based composite films was determined against foodborne pathogens *L. monocytogenes* and *E. coli*, and the results are shown in Fig. 7. The neat Car/Alg film showed no antibacterial activity against both test bacteria, and the bacterial growth was similar to the control bacterial culture (Fig. 7). However, the CD-added films showed significant antibacterial activity depending on the CD concentration. In the case of Car/Alg-CD$^{4\%}$ film, after 12 h of incubation, *L. monocytogenes* and *E. coli* were 3.5 and 2.4 log CFU/mL lower than the control, respectively. The CD-added films had higher antibacterial activity against Gram-positive bacteria than Gram-negative bacteria because allicin and polyphenols of CD can more easily penetrate the bacterial cell wall of Gram-positive bacteria due to the difference in the cell wall structure. Penetrated active compounds such as allicin and polyphenols interfere with bacterial metabolic pathways, inhibiting growth (Leontiev et al., 2018). The CDs are released from the film matrix and exert antibacterial

Table 2 Mechanical characteristics, water vapor permeability, and water contact angle of the carrageenan/alginate-based composite films

Films	Thickness (μm)	TS (MPa)	EB (%)	EM (GPa)	WVP ($\times 10^{-9}$ g.m/m^2.Pa.s)	WCA (deg.)
Car/Alg	45.7 ± 1.8^{a}	45.7 ± 2.4^{a}	4.5 ± 1.2^{a}	2.5 ± 0.3^{b}	1.7 ± 0.3^{a}	45.3 ± 2.2^{a}
Car/Alg-CD$^{1\%}$	46.9 ± 1.7^{a}	52.7 ± 1.5^{b}	4.3 ± 2.0^{a}	2.7 ± 0.1^{b}	1.6 ± 0.2^{a}	52.8 ± 2.4^{b}
Car/Alg-CD$^{2\%}$	47.4 ± 2.2^{a}	53.1 ± 2.9^{bc}	4.0 ± 1.2^{a}	2.7 ± 0.2^{b}	1.6 ± 0.3^{a}	54.7 ± 2.5^{b}
Car/Alg-CD$^{3\%}$	54.0 ± 1.0^{b}	57.2 ± 2.9^{c}	3.9 ± 0.5^{a}	1.9 ± 0.2^{a}	1.5 ± 0.3^{a}	54.4 ± 2.0^{b}
Car/Alg-CD$^{4\%}$	54.6 ± 1.4^{b}	58.6 ± 1.5^{c}	3.8 ± 1.3^{a}	2.0 ± 0.1^{a}	1.5 ± 0.2^{a}	58.2 ± 0.9^{c}

Sodium alginate (Alg), carrageenan (Car), and carbon dots (CD). Means followed by the same letter in the same column did not differ ($p > 0.05$) by Duncan's multiple range tests

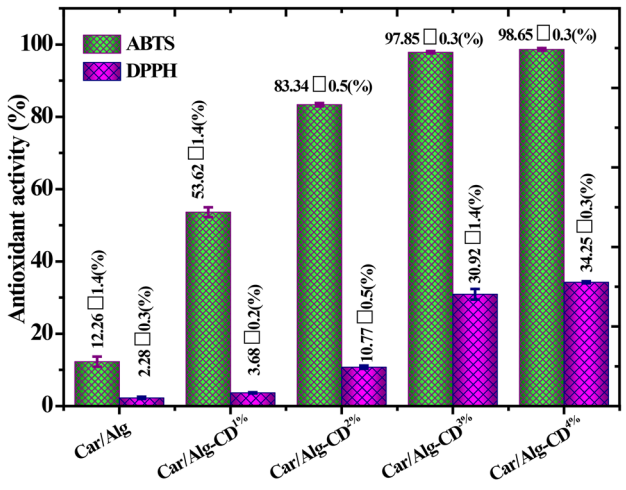

Fig. 6 DPPH and ABTS scavenging activity of the sodium alginate (Alg), carrageenan (Car), and carbon dots (CD) based Car/Alg, Car/Alg-CD$^{1\%}$, Car/Alg-CD$^{2\%}$, Car/Alg-CD$^{3\%}$, and Car/Alg-CD$^{4\%}$ films

activity against food-eating pathogens. The release properties of CDs in polymer matrices have been studied previously (Ezati & Rhim, 2022). The rate of release depends on the concentration of CD in the matrix, the type of polymer matrix, and the nature of the CD, but usually, the release is in a controlled manner and occurs in very small quantities that cannot affect the CD. However, it is still high enough to cause an antibacterial effect. A plausible mechanism for CD's antibacterial activity has been proposed (Ezati et al., 2022b). The ROS (O_2^-, OH^-, and HO_2^-) generated by CD are one of the major contributors to their antibacterial activity. These free radical groups interact with electron–hole pairs to generate hydroxyl radicals (·OH), which lead to cell wall degradation and, ultimately, cell death due to the breakdown of cellular machinery. CDs also directly interact with target molecules in the bacterial cell wall, interfering with signaling processes and intracellular metabolic activities. CD also interferes with DNA replication in microbial cells, resulting in cell death. Overall, the Car/Alg composite films with CD possessed significant bacteriostatic properties compared to the neat film and showed potential for use as antimicrobial films, especially for active packaging applications.

Application of the Films to Prevent Meat Discoloration

The quality, nutritional value, and bioactivity of food (odor, flavor, and color) are greatly influenced by UV light (< 400 nm) (Duncan & Chang, 2012). Deterioration of color properties and appearance of food is the first sign of UV-mediated spoilage. Red meat was used to test the change in surface color during storage to investigate the packaging effect of the produced CD-loaded Car/Alg-based film. Figure 8a and b show the actual view of the test samples at different intervals of UV exposure during storage under UV light at 20 °C. At the beginning of the test (Fig. 8a), the color of the test meat was identical, showing its original red color. After 30 h of storage under UV light, the control and meat covered with the neat Car/Alg film deteriorated from red to grayish with a rancid odor (Figs. 8b and 9). However, the color change, odor, or other negative observations were retarded in the meat samples covered with CD-added Car/Alg-based composite films. Among them, the Car/Alg-CD$^{4\%}$ film showed the highest efficacy in preventing the decline of the redness value of the meat samples and, therefore, was found to be the most effective UV-barrier packaging film in this experiment. Besides, the Car/Alg-CD$^{3\%}$ film was also effective due to good UV-barrier properties. These apparent color changes in the meat samples were also evaluated using the color coordinates (L, a, b, and ΔE) determined by the Chroma meter (Supporting Information Table S1). Overall, the Car/Alg-CD$^{4\%}$ film was the most effective in UV protection, along with excellent mechanical, antioxidant, and antibacterial potential, and can be effectively used in the form of UV-blocking food packaging to protect the packed food against photooxidation.

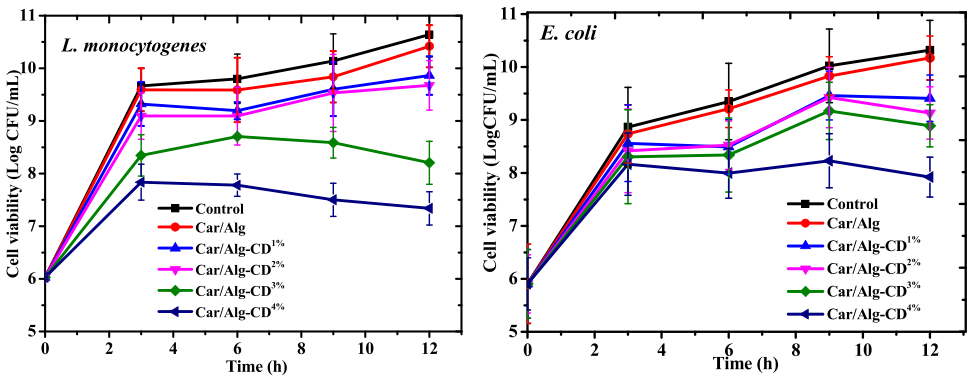

Fig. 7 Antimicrobial activity of the sodium alginate (Alg), carrageenan (Car), and carbon dots (CD) based Car/Alg, Car/Alg-CD$^{1\%}$, Car/Alg-CD$^{2\%}$, Car/Alg-CD$^{3\%}$, and Car/Alg-CD$^{4\%}$ films against *L. monocytogenes* and *E. coli*

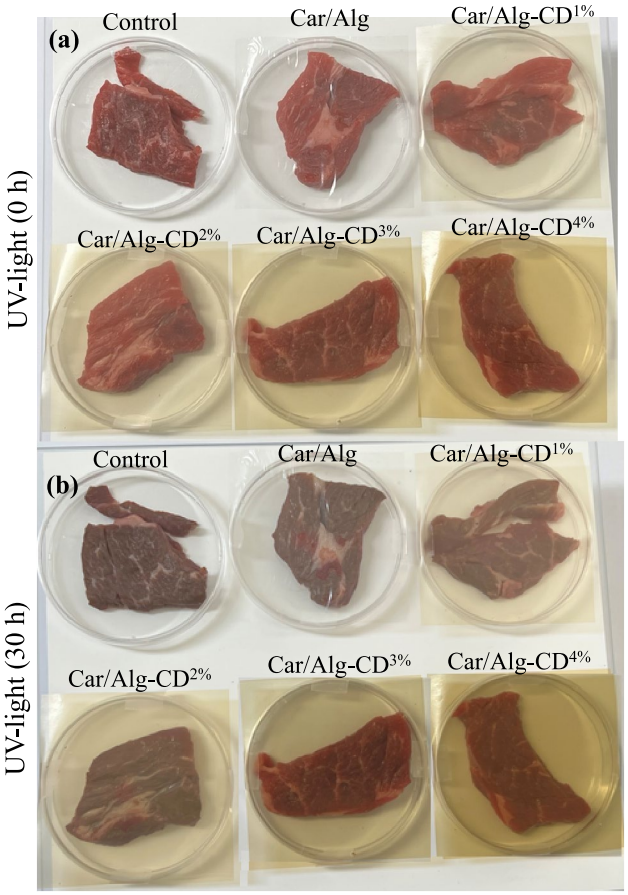

Fig. 8 Image of red meat after 30 h of UV-light exposure at 20 °C, showing uncovered sample and samples covered with the sodium alginate (Alg), carrageenan (Car), and carbon dots (CD) based Car/Alg, Car/Alg-$CD^{1\%}$, Car/Alg-$CD^{2\%}$, Car/Alg-$CD^{3\%}$, and Car/Alg-$CD^{4\%}$ films after **a** 0 h of UV-light exposure and **b** after 30 h of UV-light exposure

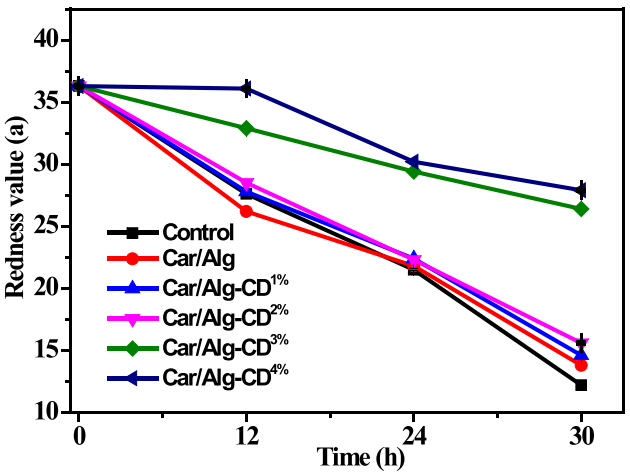

Fig. 9 Deterioration of red color of uncovered meat and meat covered by the sodium alginate (Alg), carrageenan (Car), and carbon dots (CD) based Car/Alg, Car/Alg-$CD^{1\%}$, Car/Alg-$CD^{2\%}$, Car/Alg-$CD^{3\%}$, and Car/Alg-$CD^{4\%}$ films due to exposure with UV light

Conclusions

Spherical carbon dots (CDs) with a diameter of ~ 4.8 nm and zeta potential of ~ 13 mV were prepared from garlic using a hydrothermal method and incorporated into a chitosan/gelatin polymer matrix to fabricate multifunctional composite films. The CDs were compatible with the Car/Alg polymer matrix and formed evenly mixed films. Adding CDs improved the physical and functional properties of the film. Also, the CD-added Car/Alg films blocked almost 85.1% UV-A and 99.0% UV-B radiation, exhibited potent antibacterial activity against foodborne pathogens, and showed strong antioxidant activity. The Car/Alg-based films incorporated with the 3 wt% CDs could preserve the quality by preventing the color change of the packaged meat during the 30-h storage period at 20 °C. The multifunctional Car/Alg-based films can be used in active packaging applications to protect packaged products from UV-induced photooxidation and microbial contamination.

Supplementary Information The online version contains supplementary material available at https://doi.org/10.1007/s11947-023-03048-7.

Author Contribution Ajahar Khan: conceptualization, methodology, investigation, data curation and analysis, writing—original draft. Ruchir Priyadarshi: methodology, data curation, and analysis, writing—original draft, Validation. Tanima Bhattacharya: data curation and analysis, writing—review and editing. Jong-Whan Rhim: conceptualization, writing—review and editing, supervision, project administration, funding acquisition.

Funding This work was supported by the National Research Foundation of Korea (NRF) grant funded by the Korean government (MSIT) (2022R1A2B5B02001422).

Data Availability Data supporting the findings of this study are available upon request from the corresponding author.

Declarations

Conflict of Interest The authors declare no competing interests.

References

Abdillah, A. A., & Charles, A. L. (2021). Characterization of a natural biodegradable edible film obtained from arrowroot starch and iota-carrageenan and application in food packaging. *International Journal of Biological Macromolecules, 191*, 618–626. https://doi.org/10.1016/j.ijbiomac.2021.09.141

Bahrami, A., Delshadi, R., Assadpour, E., Jafari, S. M., & Williams, L. (2020). Antimicrobial-loaded nanocarriers for food packaging applications. *Advances in colloid and interface science*, *278*, 102140. https://doi.org/10.1016/j.cis.2020.102140

Bosset, J. O., Gallmann, P. U., & Sieber, R. (1994). Influence of light transmittance of packaging materials on the shelf-life of milk and dairy products — A review. In *Food Packaging and Preservation* (pp. 222–268). Springer, Boston, MA. https://doi.org/10.1007/978-1-4615-2173-0_13

Capasso, A. (2013). Antioxidant action and therapeutic efficacy of Allium sativum L. *Molecules (basel, Switzerland), 18*(1), 690–700. https://doi.org/10.3390/MOLECULES18010690

Csapó, J., Prokisch, J., Albert, C., & Sipos, P. (2019). Effect of UV light on food quality and safety. *Acta Univ. Sapientiae, Alimentaria, 12*, 21–41. https://doi.org/10.2478/ausal-2019-0002

Đorđević, L., Arcudi, F., Cacioppo, M., & Prato, M. (2022). A multifunctional chemical toolbox to engineer carbon dots for biomedical and energy applications. *Nature Nanotechnology 2022 17:2*, *17*(2), 112–130. https://doi.org/10.1038/s41565-021-01051-7

Duncan, S. E., & Chang, H.-H. (2012). Implications of light energy on food quality and packaging selection. In *Advances in Food and Nutrition Research* (Vol. 67, pp. 25–73). Academic Press. https://doi.org/10.1016/B978-0-12-394598-3.00002-2

Duncan, S. E., & Hannah, S. (2012). Light-protective packaging materials for foods and beverages. In K. L. Yam & D. S. Lee (Eds.), *Emerging Food Packaging Technologies* (pp. 303–322). Elsevier. https://doi.org/10.1533/9780857095664.3.303

Ezati, P., Khan, A., Rhim, J.-W., Kim, J. T., & Molaei, R. (2022a). pH-responsive strips integrated with res and carbon dots for monitoring shrimp freshness. *Colloids and Surfaces B: Biointerfaces*, *221*, 113013. https://doi.org/10.1016/j.colsurfb.2022.113013

Ezati, P., Priyadarshi, R., & Rhim, J.-W. (2022b). Prospects of sustainable and renewable source-based carbon quantum dots for food packaging applications. *Sustainable Materials and Technologies*, *33*, e00494. https://doi.org/10.1016/j.susmat.2022.e00494

Ezati, P., & Rhim, J.-W. (2022). Pectin/carbon quantum dots fluorescent film with ultraviolet blocking property through light conversion. *Colloids and Surfaces B: Biointerfaces*, *219*, 112804. https://doi.org/10.1016/j.colsurfb.2022.112804

Fan, K., Zhang, M., & Chen, H. (2020). Effect of ultrasound treatment combined with carbon dots coating on the microbial and physicochemical quality of fresh-cut cucumber. *Food and Bioprocess Technology, 13*(4), 648–660. https://doi.org/10.1007/s11947-020-02424-x

Fan, K., Zhang, M., Guo, C., Dan, W., & Devahastin, S. (2021). Laser-induced microporous modified atmosphere packaging and chitosan carbon-dot coating as a novel combined preservation method for fresh-cut cucumber. *Food and Bioprocess Technology, 14*(5), 968–983. https://doi.org/10.1007/s11947-021-02617-y

Fathima, P. E., Panda, S. K., Ashraf, P. M., Varghese, T. O., & Bindu, J. (2018). Polylactic acid/chitosan films for packaging of Indian white prawn (Fenneropenaeus indicus). *International Journal of Biological Macromolecules, 117*, 1002–1010. https://doi.org/10.1016/J.IJBIOMAC.2018.05.214

Fouda, M. M. G., El-Aassar, M. R., El Fawal, G. F., Hafez, E. E., Masry, S. H. D., & Abdel-Megeed, A. (2015). k-Carrageenan/poly vinyl pyrollidone/polyethylene glycol/silver nanoparticles film for biomedical application. *International Journal of Biological Macromolecules, 74*, 179–184. https://doi.org/10.1016/J.IJBIOMAC.2014.11.040

Hashemi Tabatabaei, R., Jafari, S. M., Mirzaei, H., Mohammadi Nafchi, A., & Dehnad, D. (2018). Preparation and characterization of nano-SiO2 reinforced gelatin-k-carrageenan biocomposites. *International Journal of Biological Macromolecules, 111*, 1091–1099. https://doi.org/10.1016/J.IJBIOMAC.2018.01.116

Hoelzer, K., Moreno Switt, A. I., Wiedmann, M., & Boor, K. J. (2018). Emerging needs and opportunities in foodborne disease detection and prevention: From tools to people. *Food Microbiology, 75*, 65–71. https://doi.org/10.1016/J.FM.2017.07.006

Huang, Q., Liu, S., Li, K., Hussain, I., Yao, F., & Fu, G. (2017). Sodium alginate/carboxyl-functionalized graphene composite hydrogel via neodymium ions coordination. *Journal of Materials Science & Technology, 33*(8), 821–826. https://doi.org/10.1016/J.JMST.2016.11.003

Jafari, S. M., Ghanbari, V., Dehnad, D., & Ganje, M. (2018). Neural networks modeling of Aspergillus flavus growth in tomato paste containing microencapsulated olive leaf extract. *Journal of Food Safety*, *38*(1), e12396. https://doi.org/10.1111/jfs.12396

Kalkal, A., Allawadhi, P., Pradhan, R., Khurana, A., Bharani, K. K., & Packirisamy, G. (2021). Allium sativum-derived carbon dots as a potential theranostic agent to combat the COVID-19 crisis. *Sensors International, 2*, 100102. https://doi.org/10.1016/J.SINTL.2021.100102

Kaya, M., Khadem, S., Cakmak, Y. S., Mujtaba, M., Ilk, S., Akyuz, L., et al. (2018). Antioxidative and antimicrobial edible chitosan films blended with stem, leaf and seed extracts of Pistacia terebinthus for active food packaging. *RSC Advances, 8*(8), 3941–3950. https://doi.org/10.1039/C7RA12070B

Khan, A., Ezati, P., Kim, J.-T., & Rhim, J.-W. (2023). Biocompatible carbon quantum dots for intelligent sensing in food safety applications: Opportunities and sustainability. *Materials Today Sustainability*, *21*, 100306. https://doi.org/10.1016/j.mtsust.2022.100306

Kim, S. M., Kubota, K., & Kobayashi, A. (1997). Antioxidative activity of sulfur-containing flavor compounds in garlic. *Bioscience, Biotechnology, and Biochemistry, 61*(9), 1482–1485. https://doi.org/10.1271/BBB.61.1482

Kumar, S., Mudai, A., Roy, B., Basumatary, I. B., Mukherjee, A., & Dutta, J. (2020). Biodegradable hybrid nanocomposite of chitosan/gelatin and green synthesized zinc oxide nanoparticles for food packaging. *Foods, 9*(9), 1143. https://doi.org/10.3390/foods9091143

Kwon, S., Orsuwan, A., Bumbudsanpharoke, N., Yoon, C., Choi, J., & Ko, S. (2018). A short review of light barrier materials for food and beverage packaging. *Korean Journal of Packaging Science and Technology*, *24*(3), 141–148. https://doi.org/10.20909/kopast.2018.24.3.141

Lanzotti, V. (2006). The analysis of onion and garlic. *Journal of Chromatography A, 1112*(1–2), 3–22. https://doi.org/10.1016/J.CHROMA.2005.12.016

Leontiev, R., Hohaus, N., Jacob, C., Gruhlke, M. C. H., & Slusarenko, A. J. (2018). A comparison of the antibacterial and antifungal activities of thiosulfinate analogues of allicin. *Scientific Reports 2018 8:1*, *8*(1), 1–19. https://doi.org/10.1038/s41598-018-25154-9

Liu, Y., Qin, Y., Bai, R., Zhang, X., Yuan, L., & Liu, J. (2019). Preparation of pH-sensitive and antioxidant packaging films based on κ-carrageenan and mulberry polyphenolic extract. *International Journal of Biological Macromolecules, 134*, 993–1001. https://doi.org/10.1016/J.IJBIOMAC.2019.05.175

Mahdavinia, G. R., Rahmani, Z., Karami, S., & Pourjavadi, A. (2014). Magnetic/pH-sensitive κ-carrageenan/sodium alginate hydrogel nanocomposite beads: Preparation, swelling behavior, and drug delivery. *Journal of Biomaterials Science, Polymer Edition, 25*(17), 1891–1906. https://doi.org/10.1080/09205063.2014.956166

Makvandi, P., Wang, C., Zare, E. N., Borzacchiello, A., Niu, L., & Tay, F. R. (2020). Metal-based nanomaterials in biomedical applications: Antimicrobial activity and cytotoxicity aspects. *Advanced Functional Materials, 30*(22), 1910021. https://doi.org/10.1002/adfm.201910021

Malik, G. K., & Mitra, J. (2021). Zinc oxide nanoparticle synthesis, characterization, and their effect on mechanical, barrier, and optical properties of HPMC-based edible film. *Food and Bioprocess Technology, 14*(3), 441–456. https://doi.org/10.1007/s11947-020-02566-y

Mathew, S., Mathew, J., & Radhakrishnan, E. K. (2019). Polyvinyl alcohol/silver nanocomposite films fabricated under the influence of solar radiation as effective antimicrobial food packaging material. *Journal of Polymer Research, 26*(9), 223. https://doi.org/10.1007/s10965-019-1888-0

Mei, Y., He, C., Zeng, W., Luo, Y., Liu, C., Yang, M., et al. (2022, January 12). Electrochemical biosensors for foodborne pathogens detection based on carbon nanomaterials: Recent advances and

challenges. *Food and Bioprocess Technology*. Springer. https://doi.org/10.1007/s11947-022-02759-7

Meng, X., Zhang, M., & Adhikari, B. (2014). The effects of ultrasound treatment and nano-zinc oxide coating on the physiological activities of fresh-cut kiwifruit. *Food and Bioprocess Technology, 7*(1), 126–132. https://doi.org/10.1007/s11947-013-1081-0

Min, S., Ezati, P., & Rhim, J. W. (2022). Gelatin-based packaging material incorporated with potato skins carbon dots as functional filler. *Industrial Crops and Products*, *181*, 114820. https://doi.org/10.1016/J.INDCROP.2022.114820

Motelica, L., Ficai, D., Ficai, A., Oprea, O. C., Kaya, D. A., & Andronescu, E. (2020). Biodegradable antimicrobial food packaging: Trends and perspectives. *Foods, 9*(10), 1438. https://doi.org/10.3390/FOODS9101438

Mousavi Khaneghah, A., Hashemi, S. M. B., & Limbo, S. (2018). Antimicrobial agents and packaging systems in antimicrobial active food packaging: An overview of approaches and interactions. *Food and Bioproducts Processing, 111*, 1–19. https://doi.org/10.1016/J.FBP.2018.05.001

Nasrollahzadeh, M., Sajjadi, M., Iravani, S., & Varma, R. S. (2021). Starch, cellulose, pectin, gum, alginate, chitin and chitosan derived (nano)materials for sustainable water treatment: A review. *Carbohydrate Polymers*, *251*, 116986. https://doi.org/10.1016/J.CARBPOL.2020.116986

Njuguna, J., Pielichowski, K., & Desai, S. (2008). Nanofiller-reinforced polymer nanocomposites. *Polymers for Advanced Technologies, 19*(8), 947–959. https://doi.org/10.1002/PAT.1074

Perera, K. Y., Jaiswal, S., & Jaiswal, A. K. (2022). A review on nanomaterials and nanohybrids based bio-nanocomposites for food packaging. *Food Chemistry*, *376*, 131912. https://doi.org/10.1016/J.FOODCHEM.2021.131912

Polman, E. M. N., Gruter, G.-J. M., Parsons, J. R., & Tietema, A. (2021). Comparison of the aerobic biodegradation of biopolymers and the corresponding bioplastics: A review. *Science of The Total Environment*, *753*, 141953. https://doi.org/10.1016/j.scitotenv.2020.141953

Priyadarshi, R., Kim, S.-M., & Rhim, J.-W. (2021a). Pectin/pullulan blend films for food packaging: Effect of blending ratio. *Food Chemistry*, *347*, 129022. https://doi.org/10.1016/j.foodchem.2021.129022

Priyadarshi, R., & Negi, Y. S. (2017). Effect of varying filler concentration on zinc oxide nanoparticle embedded chitosan films as potential food packaging material. *Journal of Polymers and the Environment, 25*(4), 1087–1098. https://doi.org/10.1007/s10924-016-0890-4

Priyadarshi, R., Riahi, Z., Rhim, J. W., Han, S., & Lee, S. G. (2021b). Sulfur quantum dots as fillers in gelatin/agar-based functional food packaging films. *ACS Applied Nano Materials, 4*(12), 14292–14302. https://doi.org/10.1021/ACSANM.1C03925/ASSET/IMAGES/LARGE/AN1C03925_0007.JPEG

Puscaselu, R., Gutt, G., & Amariei, S. (2020). The use of edible films based on sodium alginate in meat product packaging: An ecofriendly alternative to conventional plastic materials. *Coatings, 10*(2), 166. https://doi.org/10.3390/COATINGS10020166

Rabinkov, A., Miron, T., Konstantinovski, L., Wilchek, M., Mirelman, D., & Weiner, L. (1998). The mode of action of allicin: Trapping of radicals and interaction with thiol containing proteins. *Biochimica Et Biophysica Acta, 1379*(2), 233–244. https://doi.org/10.1016/S0304-4165(97)00104-9

Ramos, Ó. L., Pereira, J. O., Silva, S. I., Fernandes, J. C., Franco, M. I., Lopes-da-Silva, J. A., et al. (2012). Evaluation of antimicrobial edible coatings from a whey protein isolate base to improve the shelf life of cheese. *Journal of Dairy Science, 95*(11), 6282–6292. https://doi.org/10.3168/JDS.2012-5478

Rhim, J. W. (2012). Physical-mechanical properties of agar/κ-carrageenan blend film and derived clay nanocomposite film. *Journal of Food Science, 77*(12), N66–N73. https://doi.org/10.1111/J.1750-3841.2012.02988.X

Roy, S., Ezati, P., & Rhim, J. W. (2021). Gelatin/carrageenan-based functional films with carbon dots from enoki mushroom for active food packaging applications. *ACS Applied Polymer Materials, 3*(12), 6437–6445. https://doi.org/10.1021/ACSAPM.1C01175/SUPPL_FILE/AP1C01175_SI_001.PDF

Roy, S., & Rhim, J. W. (2021). Fabrication of bioactive binary composite film based on gelatin/chitosan incorporated with cinnamon essential oil and rutin. *Colloids and Surfaces B: Biointerfaces*, *204*, 111830. https://doi.org/10.1016/J.COLSURFB.2021.111830

Saedi, S., Shokri, M., Priyadarshi, R., & Rhim, J. W. (2021). Silver ion loaded 3-aminopropyl trimethoxysilane -modified Fe3O4 nanoparticles for the fabrication of carrageenan-based active packaging films. *Colloids and Surfaces B: Biointerfaces*, *208*, 112085. https://doi.org/10.1016/J.COLSURFB.2021.112085

Saini, D., Garg, A. K., Dalal, C., Anand, S. R., Sonkar, S. K., Sonker, A. K., & Westman, G. (2022). Visible-light-promoted photocatalytic applications of carbon dots: A review. *ACS Applied Nano Materials, 5*(3), 3087–3109. https://doi.org/10.1021/ACSANM.1C04142/ASSET/IMAGES/LARGE/AN1C04142_0016.JPEG

Santos, L. G., Alves-Silva, G. F., & Martins, V. G. (2022). Active-intelligent and biodegradable sodium alginate films loaded with Clitoria ternatea anthocyanin-rich extract to preserve and monitor food freshness. *International Journal of Biological Macromolecules, 220*, 866–877. https://doi.org/10.1016/j.ijbiomac.2022.08.120

Santos, L. G., Silva, G. F. A., Gomes, B. M., & Martins, V. G. (2021). A novel sodium alginate active films functionalized with purple onion peel extract (Allium cepa). *Biocatalysis and Agricultural Biotechnology*, *35*, 102096. https://doi.org/10.1016/j.bcab.2021.102096

Schmaltz, E., Melvin, E. C., Diana, Z., Gunady, E. F., Rittschof, D., Somarelli, J. A., et al. (2020). Plastic pollution solutions: Emerging technologies to prevent and collect marine plastic pollution. *Environment International*, *144*, 106067. https://doi.org/10.1016/J.ENVINT.2020.106067

Shahabi-Ghahfarrokhi, I., Almasi, H., & Babaei-Ghazvini, A. (2020). Characteristics of biopolymers from natural resources. In *Processing and development of polysaccharide-based biopolymers for packaging applications* (pp. 49–95). Elsevier. https://doi.org/10.1016/B978-0-12-818795-1.00003-4

Sivakanthan, S., Rajendran, S., Gamage, A., Madhujith, T., & Mani, S. (2020). Antioxidant and antimicrobial applications of biopolymers: A review. *Food Research International*, *136*, 109327. https://doi.org/10.1016/J.FOODRES.2020.109327

Soltani Firouz, M., Mohi-Alden, K., & Omid, M. (2021). A critical review on intelligent and active packaging in the food industry: Research and development. *Food Research International*, *141*, 110113. https://doi.org/10.1016/J.FOODRES.2021.110113

Souza, M. P., Vaz, A. F. M., Cerqueira, M. A., Texeira, J. A., Vicente, A. A., & Carneiro-da-Cunha, M. G. (2015). Effect of an edible nanomultilayer coating by electrostatic self-assembly on the shelf life of fresh-cut mangoes. *Food and Bioprocess Technology, 8*(3), 647–654. https://doi.org/10.1007/s11947-014-1436-1

Sun, T., Tao, H., Xie, J., Zhang, S., & Xu, X. (2010). Degradation and antioxidant activity of κ-carrageenans. *Journal of Applied Polymer Science, 117*(1), 194–199. https://doi.org/10.1002/APP.31955

Uthirakumar, P., Devendiran, M., Kim, T. H., & Lee, I. H. (2018). A convenient method for isolating carbon quantum dots in high yield as an alternative to the dialysis process and the fabrication of a full-band UV blocking polymer film. *New Journal of Chemistry, 42*(22), 18312–18317. https://doi.org/10.1039/C8NJ04615H

Wang, J., & Qiu, J. (2016). A review of carbon dots in biological applications. *Journal of Materials Science, 51*(10), 4728–4738. https://doi.org/10.1007/S10853-016-9797-7

Wang, Y., Dong, X., Zhao, L., Xue, Y., Zhao, X., Li, Q., & Xia, Y. (2020). Facile and green fabrication of carrageenan-silver nanoparticles for colorimetric determination of Cu2+ and S2−. *Nanomaterials 2020, Vol. 10, Page 83*, *10*(1), 83. https://doi.org/10.3390/NANO10010083

Xu, L., Zhang, Y., Pan, H., Xu, N., Mei, C., Mao, H., et al. (1994). Preparation and performance of radiata-pine-derived polyvinyl alcohol/carbon quantum dots fluorescent films. *Food Packaging and Preservation, 13*(1), 67. https://doi.org/10.3390/MA13010067

Yousefi, H., Su, H. M., Imani, S. M., Alkhaldi, K., Filipe, C. D., & Didar, T. F. (2019). Intelligent food packaging: A review of smart sensing technologies for monitoring food quality. *ACS Sensors, 4*(4), 808–821. https://doi.org/10.1021/ACSSENSORS.9B00440/ASSET/IMAGES/MEDIUM/SE-2019-00440B_0007.GIF

Zhang, X., Xiao, G., Wang, Y., Zhao, Y., Su, H., & Tan, T. (2017). Preparation of chitosan-TiO2 composite film with efficient antimicrobial activities under visible light for food packaging applications. *Carbohydrate Polymers, 169*, 101–107. https://doi.org/10.1016/J.CARBPOL.2017.03.073

Zhao, S., Lan, M., Zhu, X., Xue, H., Ng, T. W., Meng, X., et al. (2015). Green synthesis of bifunctional fluorescent carbon dots from garlic for cellular imaging and free radical scavenging. *ACS Applied Materials and Interfaces, 7*(31), 17054–17060. https://doi.org/10.1021/ACSAMI.5B03228/ASSET/IMAGES/LARGE/AM-2015-03228E_0008.JPEG

Zhou, F., Wang, D., Zhang, J., Li, J., Lai, D., Lin, S., & Hu, J. (2022). Preparation and characterization of biodegradable κ-carrageenan based anti-bacterial film functionalized with wells-dawson polyoxometalate. *Foods, 11*(4), 586. https://doi.org/10.3390/foods11040586

Zu, F., Yan, F., Bai, Z., Xu, J., Wang, Y., Huang, Y., & Zhou, X. (2017). The quenching of the fluorescence of carbon dots: A review on mechanisms and applications. *Microchimica Acta, 184*(7), 1899–1914. https://doi.org/10.1007/S00604-017-2318-9/FIGURES/12